The Potential of the Simple Coupled Volume of Fluid and Level Set Method in OpenFoam to Elucidate the Flow of Pressure Swirl Atomizer

Abdallah Salem

Department of Mechanical and Industrial Engineering University of Wadi- Alshatti, Libya
A.Salem@wau.edu.ly

***Abstract*—In this study, the widely used open source c++ library of incompressible multiphase flows solver in OpenFoam- v1706 software, interFoam, has been modified to improve the surface tension force computation. Thus, a simple coupling of the Volume of Fluid with level set methods in the interFoam solver was implemented. The new solver, SCLSVOF, was tested against interFoam on a static droplet in a zero net gravity field to ensure robust discrete balancing between surface tension force and pressure gradient. The results have shown that the SCLSVOF method better approximates the pressure jump across the interface and yields a reduction error of almost** 8.9%**. Thus, better handling of the surface tension effect, which is essential for engineering applications with a flow of high surface tension, is achieved. Finally, the flow of a pressure swirl atomizer was simulated by the two methods. The internal flow characteristics are evaluated in terms of differential pressure between inside and outside the atomizer, discharge coefficient, and spray cone angle. The preliminary results obtained by the two methods match well with the experiment. The resulting errors using both methods, namely InterFoam and SCLSVOF methods, for the differential pressure, discharge coefficient, and spray cone angle are approximately** 2.413%**,** 3.56% **and** 1.13%**,** 9.1767%, **and** 9.4%**, respectively. The primary results ensure the robustness of both approaches in exhibiting the physical behavior of flow characteristics within the atomizer where the inertia is dominant. However, the SCLSVOF method shows better capability in capturing the disintegration mode of the swirling sheet emanating from the atomizer orifice. Consequently, SCLSVOF has good potential for investigating the atomization of pressure swirl atomizers.**

Keywords*— *Volume of Fluid, Level Set, Pressure Swirl Atomizer, interFoam, Atomization

I. INTRODUCTION

Liquid sheets, ligaments, and droplets generated by swirl atomizers gain a greater surface contact area with ambient medium and the highest surface-to-volume ratio than any other shape of jets. Therefore, a profound understanding of the internal flow characteristics and the atomization of swirling sheets leads to better expectations of the spray features, such as initial droplet size distribution and spray cone angle. Many authors studied the flow characteristics of pressure swirl atomizers. One of the early studies carried out by Taylor et al. [1] focused on the inviscid analysis of flow with the atomizer using the principle of maximum flow. An equation of the discharge coefficient was derived.

Rizk and Lefebvre [2] derived an empirical correlation for the discharge coefficient and swirling sheet angle. Although most studies concentrate on the internal characteristics, few consider the disintegration mechanism of the swirling sheet. Xiaodong and Vigor Yang [3] conducted a theoretical and numerical analysis to study the internal and external characteristics. They pointed out disturbance and stationary waves near the nozzle orifice. The analysis in our study will be restricted to the simplest form of pressure swirl atomizer, namely simplex atomizers shown in Fig. 1. Simplex atomizers are vastly used in aerospace propulsion systems, automotive engines, food processing, refrigeration units, desalination plants, and spray coating systems.

As shown in Fig. 1, the atomizer consists of a cylindrical chamber with at least one inlet tangential port. This chamber is followed by a conical section and discharging orifice. In these atomizers, the liquid flows through the tangential ports. The swirl flow within the atomizer generates a gas core inside and a conical sheet outside the atomizer.

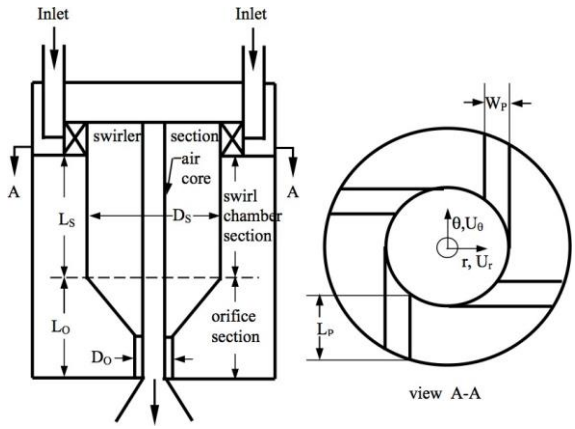

Fig. 1: Schematic of the pressure swirl atomizer tested by [4]

However, conducting a simulation of the flow field in a pressure swirl atomizer is not simple and requires two main tasks [5]. These are: tracking the interface between the liquid and the gas phases and sufficient discrete balancing between the jump in the normal stress with surface tension force. Thus, the direction in which the surface tension force acts must be well computed.

For tracing the motion of the interface, the Volume of Fluid (VOF) method first introduced by Hire et al. [6] identifies the fraction of each phase in the computational cell. The volume fraction, F, is equal to unity in computational cells fully occupied by higher-density fluid and zero elsewhere. As the interface moves, the fractional F of each cell is updated. The Volume of Fluid method has gained the advantage of being a robust mass conserving method [7]. Yet, the volume fraction F is a step function, and a reconstruction of the interface is required. This inverse problem is difficult to solve since the interface information is lost when represented by volume fraction. On the other hand, the Level Set method (LS) introduced by Dervieux et al. [8], where a sign distance function of zero value at the interface, a positive value in one phase, and a negative value in the other phase has an attractive property in defining the free surface. However, despite being a continuous function across the interface, high-velocity gradients cause the level set to be widely stretched and spread. Thus, the level set function will not maintain the property of a distance function as the interface propagates. Therefore, for large-time computations, this distortion will produce a non-uniform thickness of the interface. As a result, a random distance over which the fluid properties change and the surface tension forces are distributed is generated [9]. To overcome the drawback of each method, LS and VoF are coupled to ensure both mass conservation by VoF and better approximation of interfacial local curvature computation by LS. Many studies [9], [10], [5], and [11] showed incredible results when coupling LS with VoF in simulating the atomization of turbulent jet in quiescent gas.

Many commercial and free tools have been extensively used in recent years to simulate incompressible two-phase flows. One of these numerical codes is interFoam which has recently gained the interest and favor of many users. InterFoam becomes highly attractive compared with other commercial codes such as ANSYS and Fluent because it forms part of a suite of free, open-source C++ libraries of OpenFoam. In addition, any set of partial differential equations likely be solved numerically by resorting to a finite volume method. InterFoam uses an algebraic approach based on the re-formulation of the volume fraction advection equation to update the interface position. The main advantage of such an approach is to be computationally less costly since the geometric reconstruction of the interface is not required. Moreover, the performance of such an approach is not affected by the complexity of the computational domain. It has been shown that such an approach features an excellent mass conserving property, which is one of the most important criteria for evaluating the performance of multiphase solvers [12]. However, if the surface tension force is dominant, a less accurate discrete force balance is obtained [12]. The main source of this discrete force inconsistency is due to the poor computation of the interfacial normal and the local curvature of the interface. Thus, the main objective of this study is to improve the performance of interFoam to be more efficient in capturing the disintegration mode of the swirling sheet emanating from pressure swirl atomizers.

II. NUMERICAL MODEL

A. Volume of Fluid

The governing equations for two isothermal, incompressible, and immiscible fluids including the mass conservation, momentum, and interface capturing advection equations based on openFoam formulation [13] are given by the followings, respectively:

$$\nabla.U = 0 \tag{1}$$

$$\frac{\partial(\rho U)}{\partial t} + \nabla.(\rho U U) = \nabla.T - \nabla p_d - g.x\nabla\rho + \sigma k \nabla F \tag{2}$$

$$\frac{\partial F}{\partial t} + \nabla.(U\,F) + \nabla.[U_r F(1-F)] = 0 \tag{3}$$

Where U is the velocity vector field, p_d is the pressure , ρ is the fluid density, μ is the fluid viscosity, T is the viscous deformation tensor given by $T = \nabla.(\mu\nabla U) - \nabla U\,.\nabla\mu$, F is the volume fraction of the liquid phase , x is the position vector, g is gravitational acceleration, σ is the surface tension coefficient of the liquid phase, k is the local curvature of the interface, and U_r is the relative velocity between liquid and gas.

The surface tension force is calculated as a volume force based on the continuum force model introduced by Brackbill et al. [14].

Fluid properties such as viscosity μ and density ρ at any point in the domain are calculated as the weighted average of the volume fraction of the two fluids as the following [13]:

$$\mu = \mu_l F + \mu_g(1-F) \tag{4}$$

$$\rho = \rho_l F + \rho_g(1-F) \tag{5}$$

Where μ_l and μ_g are the viscosity of the liquid and the gas, respectively, while ρ_l and ρ_g are the density of liquid and gas, respectively [11].

The local curvature k is calculated by taking the divergence of the unit normal vector of the phase interface $\hat{n}$ as follows [9]:

$$k = -\nabla.\hat{n} = -\nabla.\left(\frac{\nabla F}{|\nabla F|}\right) \tag{6}$$

The relative velocity U_r in equation (3) must be limited to the maximum velocity field in the whole computational domain as follows [12]:

$$|U_r| = min[c_\alpha|U|, max(|U|)] \tag{7}$$

Where c_α is a compression coefficient with a value greater than 1 [15]. In our study, c_α is chosen to be 1.5.

B. Simple Coupled Level Set and Volume of Fluid (SCLSVOF)

Albadawi et al. [15] proposed a simple method of coupling the Volume of Fluid with the level set, namely SCLSVOF. In the SCLSVOF method, a new scalar field, namely level set ϕ, which represents the shortest sign distance to the interface, is added. Even though two fields define the interface, namely F

and ϕ, only F in equation (3) is advected. Albadawi et al [15] suggested that the initial value of ϕ_0 is given by:

$$\phi_0 = (2F - 1).\xi \tag{8}$$

Where ξ is a dimensionless parameter related to the mesh size $\triangle x$. It is suggested that ξ should be set to $0.75 \triangle x$ [15]. The main idea of choosing this value for ξ is to enforce the initial value of ϕ to be as close as possible to the mesh size. The value of ϕ_0 is re-distanced using the approach proposed by Sussman et al. [16] as follows:

$$\frac{\partial \phi}{\partial \tau} = sign(\phi_0)(1 - |\nabla \phi|) \tag{9}$$

The initial condition is as follows:

$$\phi(x, 0) = \phi_0(x) \tag{10}$$

Where, τ is a fictitious time and $sign$ is the sign function. Equation (9) converges to steady state either when $|\nabla \phi| = 1$ which is the property of any sign distance function or $sign(\phi_0) = 0$ which means that we are on the phase interface. The number of iterations (ϕ_{corr}) of equation (9) is limited, and has to satisfy the condition [15]:

$$\phi_{corr} = \frac{\epsilon}{\triangle \tau} \tag{11}$$

Where ϵ represents the thickness of the interface, which defines the transition region between the two phases. In our study, ϵ is equal to $1.5 \triangle x$. Once we define the smoothed level set, we re-compute the unit normal of the interface as a function of the level set as follows [9]:

$$\hat{n} = \frac{\nabla \phi}{|\nabla \phi)|} \tag{12}$$

The local curvature k is also re-computed using the continuous function ϕ by taking the divergence of equation (12) as $k = -\nabla.\hat{n}$. Moreover, the volumetric surface tension force in equation (2) that is computed by $(\sigma k \nabla F)$ is replaced by [9]:

$$F_\sigma(\phi) = \sigma k(\phi) \delta_\epsilon(\phi) \nabla \phi. \tag{13}$$

Where δ_ϵ is the smoothed Dirac function used to smooth the surface tension effect to a limited region near the interface and defined as [16]:

$$\delta_\epsilon(\phi) = \begin{cases} \frac{1}{2}[1 + cos(\frac{\pi \phi}{\epsilon})] & if\ |\phi| \leq \epsilon \\ 0 & otherwise \end{cases} \tag{14}$$

The physical properties are smoothed over a fixed thickness of the interface using the smoothed Heaviside function $H_\epsilon(\phi)$ defined as [16]:

$$H_\epsilon(\phi) = \begin{cases} 1 & If\ \phi > \epsilon \\ \frac{1}{2}[1 + \frac{\phi}{\epsilon} + \frac{1}{\pi} sin(\frac{\pi \phi}{\epsilon})] & If\ |\phi| \leq \epsilon \\ 0 & If\ \phi < \epsilon \end{cases} \tag{15}$$

Thus, the physical properties, namely the density ρ and the viscosity μ, are calculated as follows [16]:

$$\rho(\phi) = \rho_g + (\rho_l - \rho_g) H_\epsilon(\phi) \tag{16}$$

$$\mu(\phi) = \mu_g + (\mu_l - \mu_g) H_\epsilon(\phi) \tag{17}$$

Moreover, the momentum equation can be re-written as a function of the level set as follows:

$$\frac{\partial(\rho U)}{\partial t} + \nabla.(\rho U U) = \nabla.T - \nabla p_d - g.x \nabla \rho(\phi) + F_\sigma(\phi) \tag{18}$$

Details of the finite volume discretization of continuity, momentum, and volume fraction advection equations can be found in [13].

III. NUMERICAL VALIDATION OF SCLSVOF SOLVER

We validate the formulation of SCLSVOF by considering a static drop in a zero net gravity field. The exact pressure jump value $\triangle P_{Exact}$ across the interface is given by the Laplace-Younge equation as follows [12]:

$$\triangle P_{Exact} = \sigma k \tag{19}$$

Where the curvature k is calculated analytically by $\frac{1}{R}$ (R is the radius of drop), [17].

The main test case consists of a static drop positioned at the center of a square computational domain of 1×1 m. The density and kinematic viscosity of liquid and gas phases are $10^4\, kg/m^3$ and $10^{-4}\, m^2/s$, respectively. The surface tension coefficient is $\sigma = 1N/m$. Thus, the exact pressure jump is $\triangle P_{Exact} = 4$. In this test case, three uniform grids, coarse with 20×20, fine with 40×40, and finest with 80×80 cells, are considered, respectively. The numerical results are evaluated at 125 seconds with a time step $\delta t = 10^{-6}$ s. No-slip and zero gradient boundary conditions are applied to the velocity and pressure fields. Fig. 2 shows the initial set of the test.

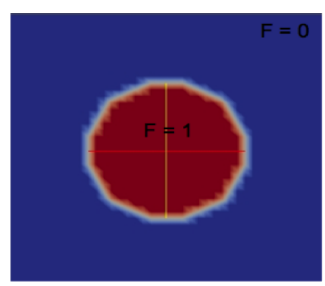

Fig. 2: Static liquid droplet in zero net gravity field

The total pressure jump $\triangle p_{total}$ and the partial pressure jump $\triangle p_{partial}$ defined by Francois et al. [17] have been evaluated as follows:

$\triangle P_{total} = P_i - P_o$, where P_i and P_o are the averaged pressure values for cells with $r \leq R$ and r > R, respectively.

$\triangle P_{partial} = P_i - P_o$, where P_i and P_o are the averaged pressure values for cells with $r \leq R/2$ and $r \geq 3R/2$,

respectively.
The relative pressure error is calculated as follows:

$$\epsilon(\triangle P)_c = \frac{|\triangle P_c - \triangle P_{Exact}|}{\triangle P_{Exact}} \tag{20}$$

Table I shows the norm errors obtained for the three grid resolutions for both SCLSVOF and interFoam solvers. The results show that the curvature computed by the two methods doesn't converge to the analytical solution as the grid resolutions increase. However, the error obtained by SCLSVOF method is almost one order of magnitude less than interFoam prediction.

TABLE I: TOTAL AND PARTIAL PRESSURE JUMP ERRORS DEFINED BY Francois et al. [17] RESULTING FROM InterFoam and SCLSVOF METHODS, RESPECTIVELY

$\epsilon(\triangle P)_c\%$	**Grid resolution**	interFoam	SCLSVOF
$\epsilon(\triangle P_{Total})\%$	20×20	20.1487	11.103
	40×40	14.76	6.42
	80×80	14.531	4.69
$\epsilon(\triangle P_{partial})\%$	20×20	14.46	1.2
	40×40	12.1	2.74
	80×80	14.214	2.81

Figs. 3 and 4 show the computed pressure along x direction for the three grid resolutions of the drop test case with interFoam and SCLSVOF methods.

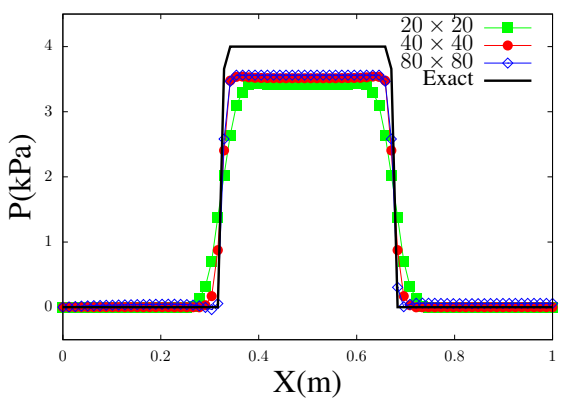

Fig. 3: Pressure variation along x-direction for the static drop with 20×20, 40×40, and 80×80 grid resolutions using interFoam method

Fig. 3 shows that the pressure jump across the interface resulting from interFoam method converges to nearly 3.5 for the three grid resolutions instead of $\triangle P_{EXACT} = 4$. On the other hand, Fig. 3 indicates that the computed curvature by the SCLSVOF method was rectified by the level set function resulting in the enhancement of the pressure jump across the static drop interface to almost 3.9 rather $\triangle P_{EXACT} = 4$ for the three grid resolutions.

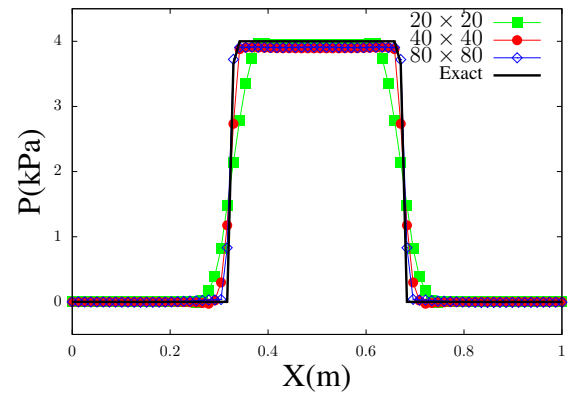

Fig. 4: Pressure variation field along x-direction for the static drop with 20×20, 40×40, and 80×80 grid resolutions using SCLSVOF method

IV. SIMULATION OF PRESSURE SWIRL ATOMIZER USING INTERFOAM AND SCLSVOF METHODS

The flow of a pressure swirl atomizer is numerically simulated using interFoam and SCLSVOF methods, respectively. The numerical simulations are compared with the large-scale atomizer tested by Xue et al. [18]. We limit our computations to 2D-axisymmetric flow to reduce the high computational cost. Moreover, we only compare the SCLSVOF method's ability to capture the disintegration of the swirling sheet emanating from the atomizer with the interFoam method.

A. The Geometrical and the Operational Conditions of the Pressure Swirl Atomizer

The pressure swirl atomizer in which the flow characteristics are simulated is the same as the one experimentally tested by Xue et al. [18] shown in Fig. 1.
Table II lists the geometrical constraints of the pressure swirl atomizer PSA.

TABLE II: GEOMETRICAL CONDITIONS OF THE PRESSURE SWIRL ATOMIZER EXPERIMENT CONDUCTED BY Xue et al. [18]

Case	Inlet Slot Area $A_p(mm^2)$	Orifice D_o, $L_o\,(mm)$	Orifice contraction angle θ
1	406	21 , 42	45°

The flow rates supplied to the atomizer are 10, 15, and 20 gallons per minute. The swirl chamber length and diameter are $L_s = 89\,mm$, $D_s = 76\,mm$, respectively.

B. 2D-Axisymmetric Physical Model

The 2D-axisymmetric model requires determining the circular slot's thickness, conserving the mass flow rate. In addition, the swirl and radial velocities in the 2D case must preserve the angular momentum and the kinetic energy of the liquid injected into the 3D atomizer. The 2D-axisymmetric model of the pressure swirl atomizer is shown in Fig. 5.

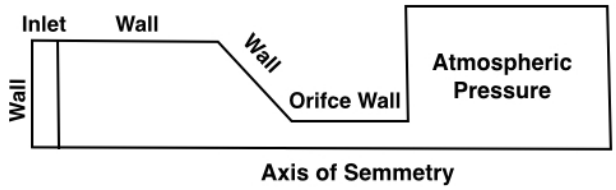

Fig. 5: Schematic of 2D-axisymmetric model of pressure swirl atomizer

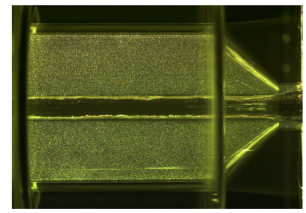

Fig. 6: PIV snapshot of the experiment of flow in the pressure swirl atomizer conducted by Xue et al [18]

The inlet swirl w_{inlet} and radial v_{inlet} velocities at the inlet of the 2D-axisymmetric model shown in Fig. 5 are given by [3]:

$$w_{inlet} = \frac{Q}{A_p}\frac{D_s - D_p}{D_s} \tag{21}$$

$$v_{inlet} = \sqrt{\left(\frac{Q}{A_p}\right)^2 - w_{inlet}^2} \tag{22}$$

Where Q is the volumetric flow rate supplied to the atomizer, D_p and D_s are shown in Fig. 1, respectively. The inlet thickness t at which the equivalent volume flow rate is flowing through the 2D-axisymmetric case is given by [3]:

$$t = \frac{Q}{\pi\, D_s\, w_{inlet}} \tag{23}$$

The number of computational cells used in all simulations is 50.000. This number is assumed to be fairly sufficient to capture the flow motion inside the atomizer where the inertia is high and the surface tension force is almost effectless. However, extremely high computational resources are needed to capture and resolve the disintegration mode and the atomization of the swirling sheet.
The discharge coefficient C_d of the pressure swirl atomizer is defined as follows [18] :

$$C_d = \frac{Q}{A_o\sqrt{\frac{2\triangle p}{\rho_L}}} \tag{24}$$

Where A_o is the nozzle orifice area and ρ_L is the liquid density, and $\triangle p$ is the differential pressure across the atomizer.
Based on the inviscid analysis of flow in pressure swirl atomizer, Rizk et al. [2] defined the discharge coefficient C_d and the spray cone angle θ° as follows:

$$C_d = 0.35\left(\frac{A_P}{D_s D_o}\right)^{0.5}\left(\frac{D_s}{D_o}\right)^{0.25} \tag{25}$$

$$\theta^\circ = 6\left(\frac{A_P}{D_o D_s}\right)^{-0.15}\left(\frac{\Delta p D_o \rho_L}{\mu_L^2}\right)^{0.11} \tag{26}$$

Where μ_L is the dynamic viscosity of the liquid phase, ρ_L is liquid density, and A_P is the area of the inlet ports.
Fig. 6 shows the PIV snapshot of the experiment of the flow in PSA conducted by Xue et al. [18].

C. Results and Discussion

Fig. 7 shows the volume fraction distribution of the water phase in the red color and the distribution of the air phase in the blue color of the three different operational conditions cases using the interFoam method.

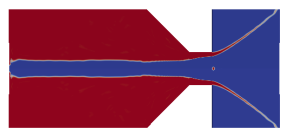

(a) Contours of Volume Fraction for Case 1 With 10 gallons/min and inlet slot area $406\,mm^2$ obtained by interFoam method

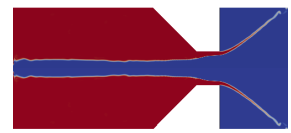

(b) Contours of Volume Fraction for Case 1 With 15 gallons/min and inlet slot area $406\,mm^2$ obtained by interFoam method

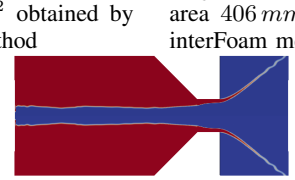

(c) Contours of Volume Fraction for Case 1 With 20 gallons/min and inlet slot area $406\,mm^2$

Fig. 7: Figs 7a, 7b, and 7b Contours of Volume Fraction for Case 1 With 10,15, and 20 gallon/min and inlet slot area $406\,mm^2$ simulated by interFoam

Fig. 8 shows the contours of the volume fraction for case 1 with 10 gallon/min and inlet slot area $406\,mm^2$ for two different time instances using the SCLSVOF method.

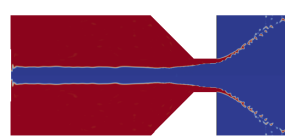

(a) Contours of volume fraction for case 1 With 10 gallons/min and inlet slot area $406\,mm^2$ at 2.5 s obtained by SCLSVOF method

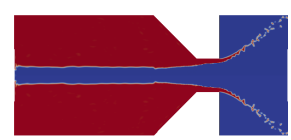

(b) Contours of volume fraction for case 1 With 10 gallons/min and inlet slot area $406\,mm^2$ at 2.55 s obtained by SCLSVOF method

Fig. 8: Figs. 8a and 8b show the Contours of volume fraction for case 1 with 10 gallon/min and inlet slot area $406\,mm^2$ obtained by SCLSVOF method

Fig. 9 shows the contours of volume fraction for case 1 with

15 gallons/min and inlet slot area $406\,mm^2$ for two different time instances resulting from the SCLSVOF method.

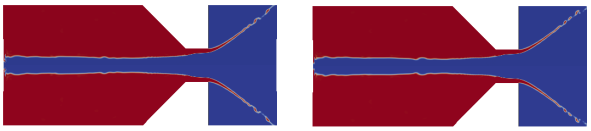

(a) Contours of volume fraction for case 1 with 15 gallons/min and inlet slot area $406\,mm^2$ at 2.5 s obtained by SCLSVOF method

(b) Contours of volume fraction for case 1 with 15 gallons/min and inlet slot area $406\,mm^2$at 2.55 s obtained by SCLSVOF method

Fig. 9: Figs 9a and 9b show the contours of volume fraction for case 1 with 15 gallons/min and inlet slot area $406\,mm^2$ obtained by SCLSVOF method

Fig .10 illustrates the differential pressure across the atomizer resulting from the experiment, InterFoam, and SCLSVOF methods. It can be noticed that the experiment and simulation results are almost compatible. The average errors obtained by interFoam and SCLSVOF methods for the three operational conditions are 7.95% and 2.413%, respectively.

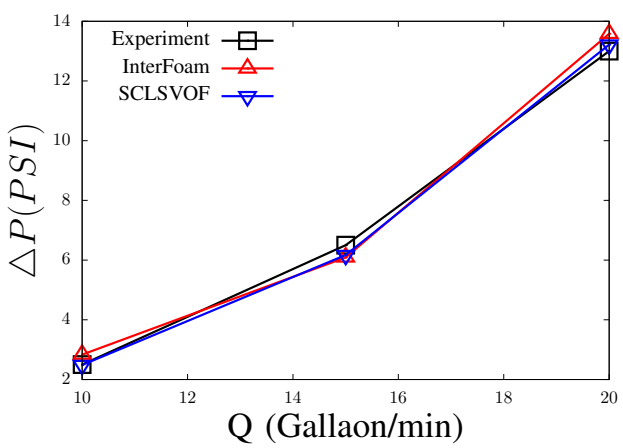

Fig. 10: The differential pressure across the pressure atomizer resulting from the experiment conducted by [18], InterFoam, and SCLSVOF

Fig. 11 shows the comparison of the discharge coefficient resulting from the solvers interFoam and SCLSVOF, respectively, with the experiment conducted by [18]. Moreover, results from the literature, namely Rizk et al. [2] are also included in the comparison.

It can be noticed that the estimation of the discharge coefficient values resulting from SCLSVOF compared to the values resulting from InterFoam is closer to the experiment outcomes. The average errors of the discharge coefficient obtained by interFoam and SCLSVOF methods for the three operational conditions are 3.56% and 1.13%, respectively. On the other hand, according to the experimental results, the predicted values from the literature finding from [2], for the values of C_d are worse compared to both the interFoam and SCLSVOF results with an average error of 29.1%.

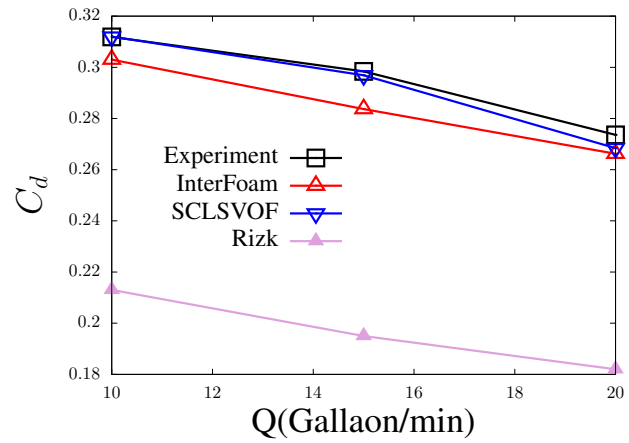

Fig. 11: Comparison of the discharge coefficient resulting from literature [2], InterFoam, and SCLSVOF methods with experiment

Fig. 12 illustrates the comparison of the spray cone angle resulting from the solvers interFoam and SCLSVOF, respectively, with the experiment conducted by [18]. The average errors of the spray cone angle obtained by interFoam and SCLSVOF methods for the three operational conditions are 9.1767% and 9.4%, respectively. On the other hand, according to the experimental results, the predicted values from the literature finding from [2], for the values of C_d are worse compared to both the interFoam and SCLSVOF results with an average error of 19.2%.

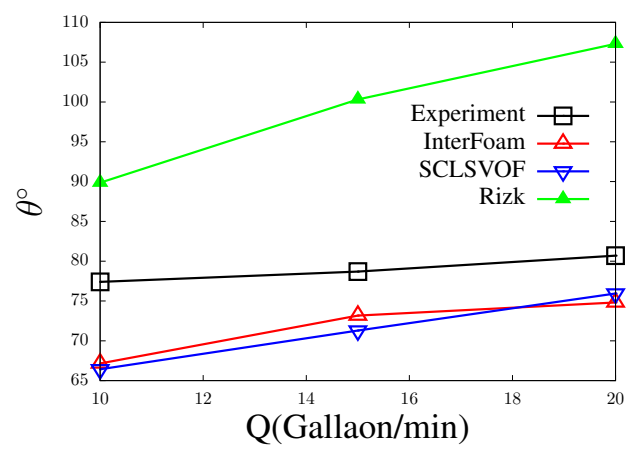

Fig. 12: Comparison of the spray cone angle resulting from literature [2], InterFoam, and SCLSVOF methods with experiment

It can be observed from Fig. 7, 8, and 9 that both methods are capable of physically capturing the internal flow motion in terms of forming an air core and swirling conical sheet. However, the swirling sheets in Fig. 8 and Fig. 9 are sharper and wavy compared to Fig. 7, which indicates the presence of

the surface tension effect [11].
Fig. 13 shows the results of the numerical simulation of the pressure swirl atomizer using the SCLSVOF method with 5×10^5 grid cells for case 1 with 10 gallons/min. This simulation aims to investigate the capability of the SCLSVOF method to elucidate the mode of disintegration of the swirling sheet for fine grid resolution.

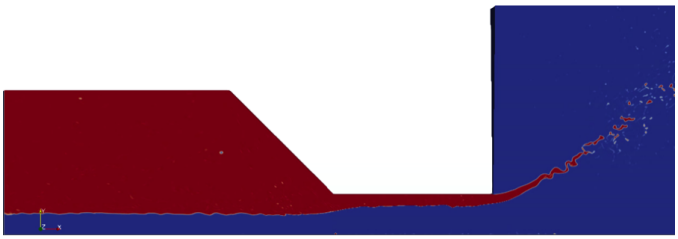

Fig. 13: Contours of volume fraction for case 1 with10 gallons/min and inlet slot area $406\,mm^2$ using SCLSVOF method and 10^5 grid resolutions

Table III shows the internal flow characteristics of the atomizer for the three operational conditions with 5×10^5 grid points using the SCLSVOF method.

TABLE III: THE INTERNAL FLOW CHARACTERISTICS OF PSA WITH 5×10^5 GRID POINTS USING SCLSVOF METHOD FOR THE THREE OPERATIONAL CONDITIONS

Q G/m	$\triangle p(PSI)$ Exp	$\triangle p(PSI)$ Sim	C_d (Exp)	C_d (Sim)	θ° (Exp)	θ° (Sim)
10	2.5	2.835	0.3119	0.303	77.4	67.16
15	6.5	6.092	0.2984	0.2837	78.7	73.12
20	13	13.58	0.2736	0.2662	80.7	74.8

It can be concluded from Table III that the internal flow characteristics are comparable with results obtained from the simulation for the same conditions when using 50.000 computational cells as shown in Fig .10, 11, 12. However, It resluts that the SCLSVOF method can maintain a sharp interface while increasing grid resolution significantly. Moreover, it remarkably captures the sheet destabilization mode (short wavy mode) and its disintegration into ligaments and droplets in comparison with its equivalent case shown in Fig 8a.

CONCLUSION AND FUTURE WORK

In this present work, a numerical method, namely SCLSVOF, has been incorporated into the source code of OpenFoam software. The new algorithm used a smooth function, namely level set to improve the computation of local interfacial curvature poorly predicted by the standered interFoam solver. The resulting error of pressure jump across the static drop interface has significantly decreased when implementing the SCLSVOF method. We also addressed the new method's potential to elucidate the flow characteristic of pressure swirl atomizers. The general features of the flow field within the atomizer where the inertia is dominant were well captured by the two methods. However, the SCLSVOF method appears more robust in handling the surface tension effect on the emanated swirling sheet than the interFoam method. Despite the need to conduct more tests on the SCLSVOF method to assess its robustness in balancing the discrete forces required for surface tension-dominated flow, this algorithm appears promising in applications involving spray and atomization phenomena. Future work will be dedicated to the detailed analysis of the effect of differential pressure on disintegration mode of the swirling sheet of the pressure swirl atomizer.

REFERENCES

[1] G. Taylor, *The Mechanics of Swirl Atomizer*. International Congress of Applied Mechanics, 1984.

[2] N. Rizk and A. H. Lefebvre, "Internal flow characteristics of simplex swirl atomizers," *Journal of Propulsion and Power*, vol. 1, no. 3, pp. 193–199, 1985.

[3] V. Y. Xiaodong Chen, "Effect of ambient pressure on liquid swirl injector flow dynamics," *Physics of Fluids*, vol. 23, 2014.

[4] J. Chinn, "The internal flow and exit conditions of pressure swirl atomizers," *Atomization and Sprays*, vol. 10, no. 2, 2000.

[5] M. Herrmann, "Detailed numerical simulations of the primary atomization of a turbulent liquid jet in crossflow," *Journal of Engineering for Gas Turbines and Power*, vol. 132, no. 6, 2010.

[6] C. W. Hirt and B. D. Nichols, "Volume of fluid (vof) method for the dynamics of free boundaries," *Journal of computational physics*, vol. 39, no. 1, pp. 201–225, 1981.

[7] A. Baraldi, M. Dodd, and A. Ferrante, "A mass-conserving volume-of-fluid method: volume tracking and droplet surface-tension in incompressible isotropic turbulence," *Computers & Fluids*, vol. 96, pp. 322–337, 2014.

[8] A. Dervieux and F. Thomasset, "A finite element method for the simulation of a rayleigh-taylor instability," in *Approximation methods for Navier-Stokes problems*, pp. 145–158, Springer, 1980.

[9] T. Ménard, S. Tanguy, and A. Berlemont, "Coupling level set/vof/ghost fluid methods: Validation and application to 3d simulation of the primary break-up of a liquid jet," *International Journal of Multiphase Flow*, vol. 33, no. 5, pp. 510–524, 2007.

[10] O. Desjardins, V. Moureau, and H. Pitsch, "An accurate conservative level set/ghost fluid method for simulating turbulent atomization," *Journal of computational physics*, vol. 227, no. 18, pp. 8395–8416, 2008.

[11] J. Shinjo and A. Umemura, "Detailed simulation of primary atomization mechanisms in diesel jet sprays (isolated identification of liquid jet tip effects)," *Proceedings of the Combustion Institute*, vol. 33, no. 2, pp. 2089–2097, 2011.

[12] S. S. Deshpande, L. Anumolu, and M. F. Trujillo, "Evaluating the performance of the two-phase flow solver interfoam," *Computational science & discovery*, vol. 5, no. 1, p. 014016, 2012.

[13] M. Damian, "S. description and utilization of interfoam multiphase solver," 2012.

[14] J. U. Brackbill, D. B. Kothe, and C. Zemach, "A continuum method for modeling surface tension," *Journal of computational physics*, vol. 100, no. 2, pp. 335–354, 1992.

[15] A. Albadawi, *On the assessment of numerical interface capturing methods for two fluid flow applications*. PhD thesis, Dublin City University, 2014.

[16] M. Sussman, P. Smereka, and S. Osher, "A level set approach for computing solutions to incompressible two-phase flow," *Journal of Computational physics*, vol. 114, no. 1, pp. 146–159, 1994.

[17] M. M. Francois, S. J. Cummins, E. D. Dendy, D. B. Kothe, J. M. Sicilian, and M. W. Williams, "A balanced-force algorithm for continuous and sharp interfacial surface tension models within a volume tracking framework," *Journal of Computational Physics*, vol. 213, no. 1, pp. 141–173, 2006.

[18] J. Xue, *Computational simulation of flow inside pressure-swirl atomizers*. PhD thesis, University of Cincinnati, 2004.